Model of ciliary clearance and the role of mucus rheology

Michael M. Norton,[1,*] Risa J. Robinson,[1] and Steven J. Weinstein[2]
[1]*Department of Mechanical Engineering, Rochester Institute of Technology, Rochester, New York 14623, USA*
[2]*Department of Chemical and Biomedical Engineering, Rochester Institute of Technology, Rochester, New York 14623, USA*
(Received 12 September 2010; published 31 January 2011; publisher error corrected 24 February 2011)

It has been observed that the transportability of mucus by cilial mats is dependent on the rheological properties of the mucus. Mucus is a non-Newtonian fluid that exhibits a plethora of phenomena such as stress relaxation, tensile stresses, shear thinning, and yielding behavior. These observations motivate the analysis in this paper that considers the first two attributes in order to construct a transport model. The model developed here assumes that the mucus is transported as a rigid body, the metachronal wave exhibits symplectic behavior, that the mucus is thin compared to the metachronal wavelength, and that the effects of individual cilia can be lumped together to impart an average strain to the mucus during contact. This strain invokes a stress in the mucus, whose non-Newtonian rheology creates tensile forces that persist into unsheared regions and allow the unsupported mucus to move as a rigid body whereas a Newtonian fluid would retrograde. This work focuses primarily on the Doi-Edwards model but results are generalized to the Jeffrey's and Maxwell fluids as well. The model predicts that there exists an optimal mucus rheology that maximizes the shear stress imparted to the mucus by the cilia for a given cilia motion. We propose that this is the rheology that the body strives for in order to minimize energy consumption. Predicted optimal rheologies are consistent with results from previous experimental studies when reasonable model parameters are chosen.

DOI: 10.1103/PhysRevE.83.011921 PACS number(s): 87.19.rh, 47.85.−g, 47.50.−d, 83.60.Bc

I. INTRODUCTION

Mucus and cilia work in tandem in the respiratory tracts of many species to clear pathogens from the body or perform other transportation functions. Lubricated by interstitial fluid, cilia beat asymmetrically to engage mucus and sweep it out of the body. Though mostly water, mucus is a chemically and rheologically complex fluid [1]. A variety of glycol-sylated proteins, called mucins, give it its intriguing mechanical properties while various additional constituents provide immunological character. Cilial dynamics and mucus rheology have attracted the scrutiny of theoreticians and experimental investigators for the past several decades. The ultimate goal of research in this area is to develop treatment strategies for the maladies that result when one more or parts of this system break down owing to disease or hereditary predisposition. Cystic fibrosis and chronic obstructive pulmonary disease are but two examples. The quantitative connection between rheology and mucus transportability is fundamental to understand and potentially treat these diseases.

Much of the initial theoretical work examining mucus clearance was an extension of studies on aquatic microorganisms that dwelled in mostly Newtonian fluids dominated by viscous forces (i.e., low Reynolds number flows). In these models, the "envelope approach" was used to simplify the problem by considering the cilia mat to be an undulating surface [2]. Many theoretical efforts attempted to extract an explicit connection between the ciliary dynamics and transport of both the mucus and the underlying interstitial fluid; Stokeslets and slender body theory were often used analysis techniques. Models often combined experimentally acquired cilia trajectories with a Newtonian bilayer geometry (in which the mucus was treated as a highly viscous fluid) to determine clearance velocities [3–6]. The focus on Newtonian fluids in these works precluded investigation of the interactions between mucus clearance and fluid rheology, now believed to be essential to mucus clearance as cited below.

The problem of a viscoelastic film propelled by an undulating layer was first considered several decades ago by using a form of the convected Maxwell fluid model and the assumption of small-amplitude deformations of the boundary wall meant to model the effect of an cilial mat [7]. The net transport of a material point in the slab was found to increase monotonically with mucus rigidity; no relationship between the viscosity of mucus and transport was extracted. More recently, transport of an Oldroyd-B fluid was examined; as in previously cited studies, a small-amplitude undulation in the cilial mat was assumed [8]. In this work, stress relaxation was predicted to reduce mechanical efficacy of mucus clearance. It was therefore posited that non-Newtonian rheologies may be favored for their ability to be tuned by the body rather than directly improve mechanical effectiveness. Though a nonlinear constitutive equation incorporating rheology was chosen, the role of its increased complexity on mucus transport compared with linear models was not elucidated. A following paper that considered a finite rigid flapper in the same medium revealed the benefits of a nonlinear constitutive equation to defeat the scallop theorem (the inability of a swimmer with only one degree of freedom to propel itself owing to the time reversibility of Stokes flow) [9]. Flow characteristics as a function of Deborah number were explored and implications of mucociliary transport were discussed. However, while the model demonstrates the fundamental importance of normal stress even in the small-amplitude regime, the results are not readily extendable to the clearance of a thin sheet in which the movers are not completely immersed in the medium.

*Present address: Department of Mechanical Engineering and Applied Mechanics, University of Pennsylvania, Philadelphia, PA 19104; mnorton@seas.upenn.edu

Green's functions or Stokeslets for fluids satisfying a linear Maxwell constitutive equation have been employed to explore the forces and velocities that result from the movement of cilia immersed in a viscoelastic mucus. The movement of the cilia is incorporated as a boundary condition by using experimental data [10]. A relaxation time that maximizes force density in a mucus film has been predicted from this technique [11]. However, note that the use of a linear model cannot account for the development of tensile forces through the action of shear [12].

Modern increases in computing power have made explicit predictions of the mucociliary interaction possible [13–15]. Rather than impose the motion of the cilia as a boundary condition, the cilia are given an internal structure intended to mimic the fibrous network and motor proteins of actual cilia. That is, the motion of the cilia themselves is part of the solution to the simulation. While these models demonstrate the ability of numerical schemes to simulate complex fluid structure interactions and understand how force is generated by the cilia, variations in rheological parameters are not explored in depth, and trends are not identified. This makes connections to experimental studies difficult.

There are a variety of experimental studies that examine specific aspects of mucociliary clearance that are particularly pertinent to the model proposed in this paper. An examination of fixed, excised rabbit trachea provides the wavelength of the metachronal wave that characterizes the release and engagement of the mucus by cilia [10]. In a separate study, the direction and speed of the metachronal wave in live cilia have been examined also [16]. These two sources disagree about the character of the metachronal wave. The former only observes antiplectic (wave propagation in a sense opposite to the direction of clearance) coordination; the latter only observes symplectic (wave propagation in the same direction as clearance). Further, it was generally found in the latter that metachronal wave velocities were larger than the clearance velocity (a condition that we find necessary to employ in our model). This disagreement no doubt indicates that the metachronal wave motion is quite complex, and that experiments have not identified and controlled all factors relevant to the relative motion of the mucus and cilia. One fact that is well established is that the ciliary beat frequency and the coordination of the metachronal wave are not connected in a straightforward manner (i.e., the wave does not exhibit simple harmonic behavior) [16,17].

For some time, it has been understood that the complex rheology of the mucus gel and the intricate dynamics and coordination of the cilia are coupled for optimal transport of the mucus. An experimental study that utilizes ciliated frog palates to study the clearance velocity of (nonmucus) viscoelastic media samples shows that transport occurs most effectively over a narrow range of storage moduli [18]. Qualitatively, this characterization implies that mucus can neither be too "solid" like or too "runny," and that only some mucus rheologies are effectively transported.

A more recent experimental study examines the transportability as a function of rheology by modifying samples with variable amounts of saline [19]. Their results show that mucus moduli measured at low frequencies have a stronger correlation with transport than material properties measured at shorter time scales. The authors highlight the ambiguity surrounding the precise mechanical role of mucus as well as the importance of two times scales in the problem: the ciliary beat frequency and the comparatively slower time associated with the wave velocity and metachronal wavelength. These works demonstrate the important effect of mucus rheology on clearance efficacy but are not able to establish a specific mechanical description of their results. Though theoretical work has advanced since this study was performed, the mechanistic role of mucus remains vague.

Three studies are now cited that report force measurements (either direct or indirect) on the cilial mat. In the first study, a spatially and temporally averaged shear stress of $\sim$1–10 Pa is calculated by analyzing an experiment in which a mucus plug moves with a constant velocity on the order of 1 μm s^{-1} against an adverse pressure difference [20]. Our interpretation of this estimate is that it may be viewed as the maximum force imparted by the cilia (used in this case to fight the pressure gradient) and already includes the adverse drag forces associated with the pericilliary fluid and imbedded cilia. More recent studies calculate the force of single cilium as they beat (without the presence of mucus) by using atomic force microscopy coupled with visual observation. The maximum force is found to be on the order of 0.1 nN [21]. Additionally, it is shown that, owing to geometric constraints of the beat cycle, this force is linearly dependent on the beat frequency [22].

Experimental studies have yielded the clearance ability of the cilia through direct observation of excised or cultured cilial mats and indirect means. Based upon experimentally acquired bulk clearance volumes and available surface area, the average flow velocity as a function of lung generation has been estimated [23]. Observation of the flow profiles in more controlled situations has also been performed by a number of researchers by using excised ciliated tissue [24–27]. Velocities on the order of 10–100 μm s^{-1} are consistently reported.

The above-cited experimental works examine many aspects of transport independently. With rare exception are there works that simultaneously examine mucus clearance, mucus rheology, and cilial dynamics. When done, these studies involve excised cilia in horizontal configurations [18,19]. Additionally, there appear to be no *in vivo* measurements of mucus clearance, no doubt owing to measurement complexity. Ideally, experiments would combine the rheological characterization of mucus across a continuum of time scales with relaxation studies [28,29] rather than at a handful of time scales [30–32], and this would be coupled to an examination of the transportability of those same specimens. Furthermore, the most elegant theoretical treatments all appear to be missing at least one piece of the clearance mechanism. We assume this because prior studies either do not reveal an optimal rheology [7,8], or they are overly limited in applicability by the viscoelastic model they choose [11].

In this paper, we propose a mechanism by which cilia motion and the non-Newtonian mucus rheology act in tandem to achieve mucus clearance in an optimal way. In order to overcome limitations of previous studies, a model of the mucociliary mechanisms is constructed that explicitly incorporates what we believe to be some of the key physical components while avoiding the complexities of more detailed simulations.

We begin with the fact that, on average, an arbitrary section of the mucus film transports in a steady-state manner. Next we consider, from the frame of reference moving with the mucus, the cyclic loading that it experiences as it traverses active and inactive regions of the cilial mat. In this portion of the analysis the rate of strain owing to moving cilia is imposed and the resulting buildup and relaxation of stress in the viscoelastic fluid is examined. Finally, we incorporate what we posit is the most dominant effect of nonlinear viscoelasticity present in the mucus film: tensile forces. By assuming a purely unidirectional flow (reasonably valid when the metachronal wavelength is large with respect to the film thickness), we are able to extract an estimate of the tensile forces that result when a fluid obeying an upper convected Maxwell (UCM) rheology is sheared. Maxwell model results are also generalized to both Jeffrey's and Doi-Edwards fluids [12]. Though nonlinear viscoelasticity has been incorporated in previous models that consider the complex flow generated by model cilium [9], its effect has not been explored in such a way that its importance in bulk transport of mucus when there are many cilia can be examined.

In tandem, these three analyses are able to predict mucus rheology (relaxation time and zero-shear-rate viscosity) as a function of average clearance velocity and other parameters such as metachronal wave and mucus dimensions. Despite its simplicity, the model is capable of predicting a rheology that maximizes stress for a given cilial motion (which is accounted for by a bulk strain rate in our analysis). Our model is unique in that it invokes an assumption that stress relaxation is necessary for positive transport of the mucus; the non-Newtonian character of mucus is an essential piece of the model. It is acknowledged at the onset that the lack of sufficient experimental data precludes our ability to validate whether our proposed mechanism is indeed correct, although it is consistent with available experimental data taken from a variety of sources. The purpose of this model, then, is to provide a framework for future theoretical and experimental exploration. The model indicates the key parameters that need to be measured and or predicted from more fundamental studies, and will guide further experiments by allowing for hypotheses based on model predictions to be tested. No doubt, more refined models can and will be generated in the future, but at this point, the level of available data precludes a more detailed theoretical study.

II. THEORY

The model we propose combines three individual fluid-mechanical analyses. (a) The first analysis yields a time-averaged overall force balance on a slab of mucus in order to establish a connection between mucus flow velocity and average force applied by the cilia. The analysis establishes the necessary condition for the cilia to sweep the mucus as a rigid body against the pull of gravity and overcome viscous drag of the underlying periciliary fluid (including the resistance of the cilia themselves). (b) The second analysis focuses on one rheological property of mucus, i.e., the relaxation time from the Maxwell model, which delays both the buildup and dissipation of shear stress. We consider a slice of the convected mucus slab that experiences the strain rate imparted by cilia for only a fraction of its length corresponding to the metachronal wave. We incorporate the the mucociliary interaction by introducing an effective strain rate and assume that all energy is imparted through shear. (c) The third analysis posits that the ability of mucus to develop tensile forces when it is sheared is essential to support regions of the mucus that are not actively sheared by cilia. A unidirectional approximation is applied to the UCM model to establish an analytical relationship between shear stress and tensile force. The Maxwell model analyses are extended to Jeffrey's and Doi-Edwards rheological equations, taking advantage of similarities in their mathematical structure.

A. Steady-state force balance on mucus

Mucus must be swept upward against gravity or in horizontal configurations must overcome the viscous drag of the periciliary fluid whose properties are convoluted with the cilia imbedded in them. The cilia must supply the forces necessary to propel the mucus. For the purposes of the force balance to follow, the mucus is modeled as a rigid body, despite the fact that there is some mucus deformation owing to the cilia. This is justified because the viscosity of the mucus is extremely large compared with that of the periciliary layer (PCL) on which the mucus rests (Fig. 1). Additionally, in this model, the precise details of the cilia motion in the PCL are neglected. The effect of the cilia motion is incorporated via propulsive force and a drag force, both of which act on the interface between the mucus body and the PCL. The stresses that exist *within* the mucal layer owing to the cilia motion will be considered in Sec. II B. Because of the repeating nature of the metachronal wave, the control volume is drawn in over one complete wavelength unit in such a way that forces incurred when cutting through the mucus film are equal and opposite, and thereby cancel.

Consider a finite rectangular slab of mucus of thickness, h_M, length ξ, and width w, riding over a PCL against the action of gravity of magnitude g_x (Fig. 1). If the mucus slab is to maintain constant velocity V_M, then all external forces on the moving slab must balance:

$$\sum F_x = 0 = F_{\text{cilia}} - F_{\text{drag}} - F_{\text{mucus}}. \tag{1a}$$

The length is chosen to be equal to that of the metachronal wavelength ξ. The periodic nature of the metachronal wave

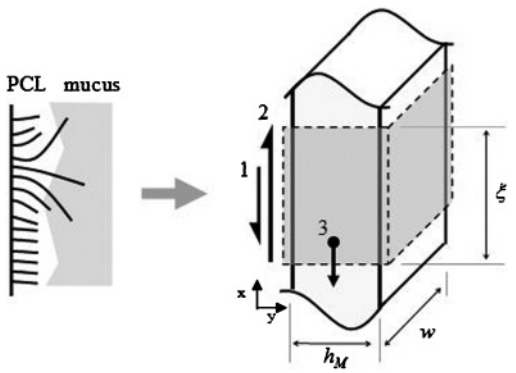

FIG. 1. Schematic of rigid-body problem. The relevant forces are labeled as (1) drag, (2) average stress applied by cilia, and (3) weight of mucus.

allows us to assume that stresses which exist at the top and bottom of our free body are equal and opposite. Note that in Fig. 1, the x-y coordinate system is as indicated, and the motion of the slab is upward. The two forces opposed to the propulsive force are the body force owing to the weight of the mucus and the frictional drag of the PCL. The body force is given as

$$F_{\text{mucus}} = \rho g_x h w \xi. \tag{1b}$$

The frictional drag of the PCL, although intuitively an obvious contribution, is difficult to express mathematically. Modeling the PCL has been a topic of interest in several previous works [6,33–35]. When active, the densely packed cilia directly engage the mucus and propel it. Cilia that are inactive or execute their recovery stroke, however, impose a drag on the mucus layer above. Thus the PCL can be thought of as a continuous distribution of forces, some of which are beneficial and others which are detrimental. It has been proposed by some investigators that this drag be modeled by assuming that the PCL behaves as a porous medium [36]. At present we are, however, uninterested in the subtleties of this region and lump the positive and negative effects of the cilia into two stresses. The first incorporates the effect of the drag of the PCL augmented by the cilia themselves, and is assumed to be proportional to the velocity through a frictional coefficient μ. We expect this value to be quite high as to account for the fact that the cilia are closely packed; however, because of the aforementioned complexities, we do not attempt to predict its value through a theoretical treatment. A value for the coefficient will be estimated later in the analysis when we compare the rheologies predicted by our model with experimentally acquired data:

$$F_{\text{drag}} = \tau_{\text{drag}} w L = \mu V_M w \xi. \tag{1c}$$

The beneficial stress, denoted by $\langle \tau \rangle$, is a shear force imparted to the mucus slab by the cilia; the brackets indicate that the quantity is spatially and temporally averaged:

$$F_{\text{cilia}} = \langle \tau \rangle w \xi. \tag{1d}$$

Substituting all of the components into the force balance yields the following equality:

$$w\xi(\langle \tau \rangle - V_M \mu - \rho g_x h) = 0. \tag{1e}$$

Solving for the average stress yields the desired result of the first analysis:

$$\langle \tau \rangle = V_M \mu + g_x \rho h. \tag{1f}$$

The resulting Eq. (1f) tells us that for a fixed mucus velocity, the average stress is entirely known if we select a friction coefficient. In Secs. II B and II C we will impose more complex restrictions on $\langle \tau \rangle$; however, we will continue to enforce the requirement of rigid-body motion throughout the analysis.

B. Stress development

We now examine how stress builds in the mucus owing to the motion of the cilia and quantify it via a simplified analysis. The goals of the analysis to follow are (1) to establish a relationship between the average strain rate imparted by the cilia and the average shear stress developed in the mucus, and (2) to determine the instantaneous shear stress in the mucus layer. A proper choice of reference frame will allow us to examine the derived stress as either a function of time or position within the metachronal wave. The shear stress itself does invoke tensile stresses in the mucus, which will be examined in Sec. II C.

Literature cited in Sec. I indicates that a distinguishing rheological property of mucus is its tendency to behave as an elastic solid on short time scales. A universal constitutive equation between stress and strain for viscoelastic media does not exist. By contrast, there are many nonelastic fluids that can be described by a Newtonian constitutive equation in which its key parameter, the viscosity, is a material property that can be measured. The material property character assures that the measurement of viscosity can occur in a system different from the particular configuration being analyzed (e.g., in a viscometer or rheometer). The rheology of mucus is complex enough that a single constitutive equation describing its stress-strain relationship has not yet been established in terms of fundamentally measurable material quantities. Therefore, phenomenological models that incorporate the elastic character of the mucus must be assumed, although the parameters involved may not in fact be material parameters. Providing a model that accounts for stress relaxation versus time is the most fundamental building block. Mucus, as other organic polymeric solutions, is capable of additional behaviors beyond time-scale dependence whose implications are beyond the scope of the current paper [28,29,37].

When mucus is deformed abruptly by cilia, the relationship between stress and strain tends toward the elastic behavior of a solid. The simplest viscoelastic fluid model that allows for elastic behavior on short time scales is the Maxwell constitutive equation, which relates the rate of strain and stress. The Maxwell model should be thought of as the addition of elasticity to a Newtonian fluid model; it can be represented schematically as a viscous dashpot of viscosity η_0 (commonly referred to as the zero-shear-rate viscosity) and a Hookean spring with spring constant G in series as shown in Fig. 2. This constant G is often related to the viscosity and relaxation time, λ, of the material, as $G = \eta_0/\lambda$.

The differential equation describing the relationship between stress and strain rate is given as

$$\lambda \frac{d\tau}{dt} + \tau = \eta_0 \dot{\gamma}, \tag{2}$$

where τ and $\dot{\gamma}$ are the generally time-dependent stress and strain rate, respectively. A cursory inspection of the equation shows that in cases of small relaxation times ($\lambda \to 0$), Eq. (2) reduces to a Newtonian relationship between stress and strain.

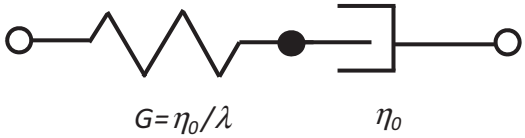

FIG. 2. Schematic of the Maxwell fluid element. The rigidity of the elastic element G is defined in terms of the relaxation time λ and zero-shear-rate viscosity η_0; this notation is common in texts.

TABLE I. Parameters for various rheological models in Eq. (2b). The subscripts 1 and 2 refer to relaxation time and retardation time, respectively. The retardation time must always be less than the relaxation time [12]; β is therefore always less than 1. If λ appears without a subscript in the body of the text, relaxation time is implied.

Model	α	β	δ
Maxwell	1	1	$1/\lambda_1$
Jeffrey's	1	$(\lambda_1 - \lambda_2)/\lambda_1$	$1/\lambda_1$
Doi-Edwards	$96/\pi^4$	1	π^2/λ_1

In the limit of large relaxation times $\lambda \gg 1$, holding fixed the rigidity of the elastic element, $G = \eta_0/\lambda$, Eq. (2) reduces to Hooke's law.

Rheological studies of mucus often consist of the automated acquisition of the real and imaginary parts of the frequency-dependent dynamic modulus, the storage, and loss modulus. To truly characterize mucus by this method, the moduli need to be acquired at a continuum of time scales. Unfortunately, most studies in the literature report the moduli at only a handful of time scales that are orders of magnitude apart [30–32]. These data points are insufficient to reconstruct the rheological profile of mucus. For this reason, we turn our attention to two studies. One has fit rheological parameters for the Jeffrey's model to a stress relaxation curve acquired by using a standard cone and plate rheometers [29]. A second, more recent, study utilizes aunique microrheological technique by using paramagnetic beads to yield a relaxation time for the Doi-Edwards model [28]. Both models are mathematically similar to the Maxwell model [Eq. (2)], so we can generalize our solution and thus make our final model compatible with these studies and make comparison more transparent. This is accomplished by introducing the parameters δ, α, and β, which are defined in Table I:

$$\delta\tau + \frac{d\tau}{dt} = \alpha\eta_0\left[\delta\dot{\gamma} + (1-\beta)\frac{d\dot{\gamma}}{dt}\right]. \tag{3a}$$

We are interested in the amount of stress that cilia can impart into mucus as it is convected in the respiratory tract. Here, we will use the fact that the collective beating of cilia possesses wavelike organization to impose periodic conditions on an element of mucus as it continuously builds and dissipates stress. While the advent of efficient numerical solvers has made explicit inclusion of complex cilia beat patterns a feature in previously cited works, we move forward by using an effective strain rate to lump together the collective beating of the cilia. That is, our analysis focuses on the bulk transport characteristics of the mucus.

As indicated in Fig. 3, the problem is examined from the perspective of a parcel of mucus as it moves at the velocity of the mucus, V_M. The frequency of the switching between "on" and "off" regions is therefore a function of the metachronal wave velocity V_W, and wavelength ξ and average mucus convection velocity. We note that the phase speed and wavelength of the metachronal wave, and the beat frequency of the cilia, are not linked together as they might be if the wave exhibited simple harmonic behavior [16,17].

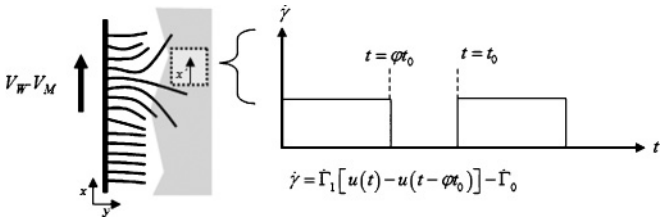

FIG. 3. Strain rate imposed on an element of mucus that travels along the mucus-PCL interface. The element of mucus is observed from a reference frame x' that moves at the average clearance velocity of mucus V_M.

From a frame of reference moving at the average clearance velocity of the convected mucus, the cilial mat has a wave velocity of

$$V_{W,\mathrm{rel}} = V_W - V_M. \tag{3b}$$

The total time for a strain cycle, t_0, is given by

$$t_0 = \frac{\xi}{V_W - V_M}, \quad V_W > V_M, \tag{3c}$$

where ξ is the wavelength of the metachronal wave. The reason for the restriction on the relative velocity between the clearance velocity and wave velocity will become apparent in the Sec. II C. For now, it suffices to say that our postulate for rigid-body clearance of the mucus relies on a favorable distribution of stresses that only occurs if the wave speed travels at a velocity greater than the clearance velocity in the same direction. This transformation between time and position is only possible when the velocity of the wave does not equal the mean velocity, $V_W \neq V_M$.

We assume that input strain rate comprises two components that can be superimposed owing to the linearity of the Maxwell model. The cilia apply a constant strain rate $\dot{\Gamma}_1$ throughout the course of its interaction with the mucus defined by using the step function $u(t)$. Additionally, a strain rate $\dot{\Gamma}_0$ that uniformly retards the motion of the mucus slab is imposed by the periciliary fluid. The input strain rate is therefore given by

$$\dot{\gamma} = \dot{\Gamma}_1[u(t) - u(t - \varphi t_0)] - \dot{\Gamma}_0. \tag{3d}$$

The duration of the interaction between the cilia and the mucus is represented as some fraction φ of the total time to traverse the entire wavelength. We argue that it can be no more than 0.5 because at least 0.5 of the cilia must be recoiling from the active part of their stroke at any given time, but otherwise leave the fraction variable in the analysis. Periodicity is enforced by requiring the stress in the mucus element at the end of the metachronal wavelength equal to the stress at the beginning:

$$\tau_{xy}(t = 0) = \tau_{xy}(t = t_0) = \tau_0, \tag{3e}$$

where τ_0 is the initial stress. This stress is part of the solution of the problem, determined by the enforcing equation (3e). The solution of the system of Eqs. (3) by using Laplace transforms yields the following time-dependent solution for stress (the full derivation is presented in Appendix A):

$$\tau_{xy}(t) = \begin{cases} \alpha(\eta_0\dot{\Gamma}_1)(1-\beta e^{-\delta t}) + \tau_0 e^{-\delta t} - \alpha(\eta_0\dot{\Gamma}_0), & t \in [0,\varphi t_0], \\ e^{-\delta t}[\alpha(\eta_0\dot{\Gamma}_1)(\beta e^{\delta\phi t_0} - \beta) + \tau_0] - \alpha(\eta_0\dot{\Gamma}_0), & t \in [\varphi t_0, t_0], \end{cases} \tag{4a}$$

where

$$\tau_0 = \alpha(\eta_0\dot{\Gamma}_1)\beta\frac{(e^{\delta\phi t_0}-1)}{(e^{\delta t_0}-1)}. \tag{4b}$$

The results [Eqs. (4)] are general for the three similar viscoelastic fluid models: Maxwell, Jeffrey's, and Doi-Edwards; parameters are chosen in accordance with Table I. A sketch of Eqs. (4) is shown in Fig. 4 for the Maxwell fluid case.

Equations (3a) and (3b) provide the stress state of an infinitesimal amount of mucus as it is convected at velocity V_M. The solution for stress as a function of time is then averaged over the period of the cilia beat cycle. This is done in order to relate the stress described by the viscoelastic model back to the average shear stresses imposed by the mucus and periciliary fluid in the steady-state force balance discussed in Sec. II A. The integral average of the stress result [Eqs. (4)] is expressed as

$$\frac{1}{t_0}\int_0^{t_0}\tau_{xy}(t)\,dt = \alpha\eta_0\dot{\Gamma}_1\varphi - \alpha\eta_0\dot{\Gamma}_0. \tag{5a}$$

We recognize the first term on the right-hand side of Eq. (5a) as the average active shear generated by the cilia $\langle\tau\rangle$; the second term is the stress imposed on the mucus owing to the periciliary fluid (which translates into an internal stress in the mucus). For reference, then, we write

$$\alpha\eta_0\dot{\Gamma}_1\varphi - \alpha\eta_0\dot{\Gamma}_0 = \langle\tau\rangle - \tau_{\text{drag}}, \tag{5b}$$

where

$$\langle\tau\rangle = \alpha\eta_0\dot{\Gamma}_1\varphi, \tag{5c}$$

$$\tau_{\text{drag}} = \alpha\eta_0\dot{\Gamma}_0. \tag{5d}$$

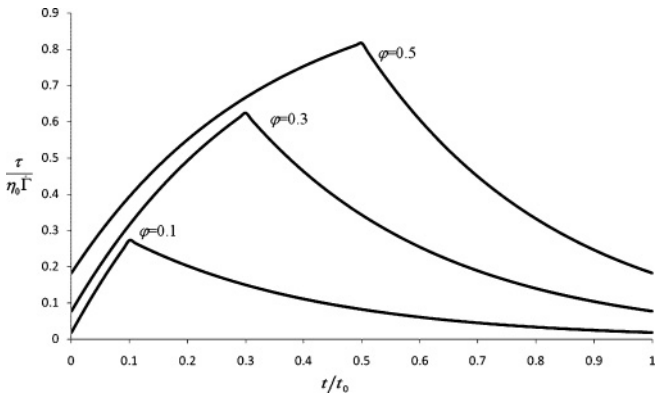

FIG. 4. Transient buildup and relaxation of shear stress within an element of mucus as it is convected for three different active fractions, 0.1, 0.3, and 0.5, as described by Eqs. (4). Parameters from Table I for the Maxwell model are used with a relaxation time $\lambda_1 = 0.3$ s.

We can define the contribution to the strain rate in the mucus owing to the drag forces of the periciliary region by combing Eqs. (1c) and (5d) to yield

$$\dot{\Gamma}_0 = \frac{V_M\mu}{\alpha\eta_0}. \tag{5e}$$

The results shown in Eqs. (5c)–(5e) are the desired relationships from our derivation. The physics of the result presented in Eq. (5b) can be assessed by considering the original force balance [Eq. (1e)]. The difference between the productive stress generated by the cilia and their own drag is the amount of stress left to do work, i.e., lift the mucus against gravity.

Note that expression (5c) is devoid of δ and β. It is therefore independent of the transient details of the applied strain rate. In other words, the viscoelastic character of the mucus does not change the relationship between the effective strain rate and stress once transience has been averaged out. The inability of these models to produce results that differ from the Newtonian stress on average is a consequence of the linearity of the models and the periodicity of the boundary conditions.

C. Continuity of tensile stress

In addition to the stress buildup and decay exhibited by viscoelastic media, tensile stresses readily develop in polymeric solutions. This ability is responsible for die-exit swell and rod-climbing phenomena as well as the ability of melts and polymeric solutions to be spun into fibers. We propose that tensile forces not only arise in the mucus flow, but play a fundamental role in maintaining positive transport in spite of the heterogeneity of the strain supplied by cilia. Thus, we will use this postulated mechanism in order to further restrict the rheological parameters λ and η_0. During the first portion of the wave cycle, the cilia actively strain the mucus toward the underside of the mucus slab and thereby invoke shear stresses, and during the latter portion of the cycle, they do not (Fig. 5). Tensile stresses generated during cilia contact must support the portion of the mucus that has lost this contact in the latter part of the cycle so as to maintain the assumed rigid-body transport.

A model is required to incorporate this physics; we require a linkage between the imposed shear from the cilia to tensile stress in the mucus. The simplest model that predicts the existence of tensile stresses is an extension of the Maxwell model considered in Sec. II B. The UCM model allows for the convection of the stress tensor by replacing the time derivative in Eq. (2a) with the convected derivative as

$$\lambda\tau_{(1)} + \tau = \eta_0\dot{\gamma}_{(1)}, \tag{6a}$$

where

$$\tau_{(1)} = \frac{D\tau}{Dt} - \{\tau \cdot \nabla v\}^T - \{\tau \cdot \nabla v\}, \tag{6b}$$

$$\gamma_{(1)} = (\nabla v)^T + (\nabla v). \tag{6c}$$

This model suffers from quantitative inaccuracies [12]. However, it captures the essential physics for the purposes of our model. Again, Eq. (6a) can be generalized to the other rheological models considered by using the notation given in Table I:

$$\delta\tau + \tau_{(1)} = \alpha\eta_0[\delta\gamma_{(1)} + (1-\beta)\gamma_{(2)}], \tag{6d}$$

$$\gamma_{(2)} = \frac{D}{Dt}\gamma_{(1)} - \{(\nabla v)^T \cdot \gamma_{(1)} + \gamma_{(1)} \cdot (\nabla v)\}. \tag{6e}$$

To our knowledge, a convected form of the Doi-Edwards model has not been proposed. Therefore, because its linear form is similar to that of the Maxwell model, we choose to extend it to large deformations by using the same convected derivative present in the UCM. Inclusion of the more general time derivative in Eqs. (6) makes all but the simplest flows analytically intractable. Similarly, we introduce the convected form of the rate of strain tensor to extend this part of the analysis to the convected Jeffrey's (also referred to as an Oldroyd-B fluid).

To simplify the analysis, we assume that the fundamental behavior of one cycle repeats for all other regions experiencing metachronal coordination. The frame of reference for the analysis is taken to be moving with the velocity of the metachronal wave, V_W. In this frame of reference the mucus slab has a velocity $V_M - V_W$. We utilize a small slope approximation, and assume that changes in the velocity and stress fields in the direction of flow are small as the mucus convects:

$$\tau_{xy} = \alpha\eta_0\frac{\partial u_x}{\partial y}, \tag{7a}$$

$$\tau_{xx} = \frac{2\alpha\eta_0(\beta-1)}{\delta}\left(\frac{\partial u_x}{\partial y}\right)^2 + \frac{2}{\delta}\tau_{xy}\frac{\partial u_x}{\partial y}. \tag{7b}$$

The relationship (7b) implies that a fully developed steady flow in Cartesian coordinates invokes normal stresses when there is shear but they are latent; they do not change the flow field compared with a Newtonian analog. However, tensile forces are present, and can be extracted in terms of the known flow. Simplifications of the constitutive relationship which lead to this conclusion are shown in the Appendix B [12]. The total tensile stress generated by the active region is calculated by assuming a stress profile that does not vary across the cross section of the mucus film:

$$\alpha\eta_0\frac{\partial u_x}{\partial y} = \tau_{xy}(x''), \tag{7c}$$

where we have defined the spatial coordinate that moves with the metachronal wave x'' in the following way:

$$x'' = t(V_W - V_M), V_W > V_M. \tag{7d}$$

By using Eqs. (7), the normal stress distribution in the actively sheared region τ_{xx} is given by the following equation, where τ_{xy} is the building and decaying shear stress given by Eqs. (4):

$$\tau_{xx}(x'') = \frac{2\beta}{\alpha\eta_0\delta}\tau_{xy}(x'')^2. \tag{8}$$

The resulting equation (8) is strictly valid only when the ratio of the mucus film thickness to that of the metachronal wavelength is small in accordance with the small slope assumption.

Next, we obtain an expression for the total force owing to tensile stresses that can be used in an appropriately drawn free body. We assume that the fundamental unit shown here repeats along the mucus; mucus flows into and out of the control volume at a velocity $V_W - V_M$.

As it flows through this control volume, the stress built while the mucus was actively strained decays. We integrate Eq. (8) over the cross-sectional area of the mucus (width w and height h_M) to find the total tensile force F_T at any given location x along the mucus:

$$F_T(x'') = \frac{2\beta}{\alpha\eta_0\delta}\tau_{xy}(x'')^2 w h_M. \tag{9}$$

A force balance on the inactive portion of the flow includes three contributions (Fig. 5): the difference between the tensile forces on the top and bottom of the unstrained region (at $x'' = 0$ and $x'' = \xi\varphi$), the shear at the mucus-PCL interface, and the weight of the mucus:

$$\sum F_x = [F_T(x'' = \varphi\xi) - F_T(x'' = \xi, 0)] - F_{\text{drag}} - F_{\text{weight}} = 0. \tag{10}$$

We note that if $V_M > V_W$, x'' and the shear stress profile would be oriented in the opposite sense. Thus, the difference between the tensile forces on the top and bottom of the inactive region only results in a productive tensile force for the case when $V_W - V_M$ is a positive quantity; this is the reason for our restriction cited earlier in Eq. (2d). That is, in our model

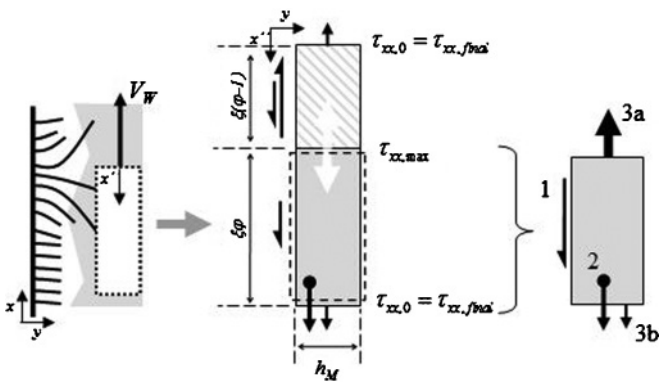

FIG. 5. Problem schematic for a unidirectional flow of a UCM fluid. The forces to be balanced on the "inactive" region (gray) are labeled as (1) drag, (2) weight, (3a) beneficial tensile stress $\tau_{xx,\max}$, (3b) detrimental tensile stress $\tau_{xx,0} = \tau_{xx,\text{final}}$. The spatial coordinate x'' denotes the moving reference frame within which this free body is drawn. Note that from this perspective the mucus enters through the top of the control volume and exists through the bottom at velocity $V_W - V_M$. For this reason, $x'' = 0$ corresponds with $t = 0$ in result shown in Eqs. (4) and Figs. 3 and 4.

we can only predict clearance when wave coordination is symplectic. This is contrary to some but not all observations of cilial coordination, [10,16] an issue to be discussed in Sec. IV.

In our simplified picture of the dynamics we continue to use the effective drag coefficient, which assumes *a priori* that the region that is no longer actively sheared continues to evacuate at the constant clearance velocity V_M. The stress at the beginning and end of the unstrained region is given by the stress relationship derived earlier by considering the buildup and relaxation of stress within a parcel of mucus as it is convected at an average velocity V_M. The final stress balance that results from substituting Eqs. (9) and (4) into Eq. (10) is stated below:

$$\frac{2\beta}{\alpha\delta\eta_0}h_M\left\{\left[\alpha\eta_0\dot{\Gamma}_1(1-\beta e^{-\delta\varphi t_0})+\alpha\eta_0\dot{\Gamma}_1 e^{-\delta\phi t_0}\beta\left(\frac{e^{\delta\varphi t_0}-1}{e^{\delta t_0}-1}\right)-\tau_{\text{drag}}\right]^2-\left[\alpha\eta_0\dot{\Gamma}_1\beta\left(\frac{e^{\delta\varphi t_0}-1}{e^{\delta t_0}-1}\right)-\tau_{\text{drag}}\right]^2\right\}$$
$$-(1-\varphi)\xi\langle\tau\rangle=0, \tag{11}$$

where the time for an element of mucus to traverse the metachronal wavelength t_0 given by Eq. (3c) is used for compactness.

Alone, this balance is not capable of examining the effect of rheology on mucus clearance. Even if all of the geometric variables are fixed (active fraction, mucus film thickness, etc.), there is still the unknown effective strain rate and the rheological parameters. The goal of the next section will be to combine the models in a way that yields an interpretable result and reveals useful relationships between the rheological parameters, clearance, and the action of cilia.

D. Final model

So far we have examined the problem from three self-consistent points of view. First, the relationship resulting from Eqs. (1) in Sec. II A provides a steady-state force balance that connects the spatially and temporally averaged relationship between the stress exerted by the cilia and the velocity of the mucus. It tells us that for a fixed mucus velocity, the average stress is entirely known if we select a friction coefficient; Eq. (1f).

Second, in Sec. II B, we consider an element of mucus as it was convected from a region strained by the cilia to a region that was unstrained. Because of relaxation time, stress in the mucus slowly builds and then relaxes. We use this model for two purposes. By averaging over a period of the mucus' stress cycle, Eqs. (4), we arrive at relationship between an effective strain rate imparted by the cilia and the average stress [Eqs. (5)].

We use the same relationship [Eqs. (4)] between stress and time (or position) in yet another force balance where we examine only the unstrained portion of the mucus. In this reference frame, we travel with the metachronal wave for convenience. We introduce the convected time derivative to expand our viscoelastic models and estimate a relationship between tensile stresses and the established shear stress field, Eq. (11).

Now we wish to assemble these three analyses in a way that reveals the fundamental relationships between clearance velocity, strain by cilia, and the rheological parameters of the mucus. Algebraically, it will be most convenient to first arrive at an expression for η_0 as function of λ. In order to gain physical insights, we will then examine the ratio between average shear stress (fixed for a given velocity) and strain rate (as a function of a relaxation time). Though not a dimensionless quantity, we posit that this ratio defines a kind of efficiency of the system as it describes how much shearing is required to achieve a given shear stress in the film. To accomplish these goals, we first note that the factor $\alpha\eta_0\dot{\Gamma}_1$ can be eliminated from Eq. (11) by using Eq. (5c). This leaves one instance of η_0, which can then be solved for directly:

$$\eta_0=\frac{2\beta h_M}{\xi\delta\alpha}\frac{\langle\tau\rangle[(C_1)^2-(C_2)^2]+2\varphi\tau_{\text{drag}}(C_2-C_1)}{\varphi^2(1-\varphi)}, \tag{12a}$$

$$C_1=\left[(1-\beta e^{-\delta\varphi t_0})+e^{-\delta\phi t_0}\beta\left(\frac{e^{\delta\varphi t_0}-1}{e^{\delta t_0}-1}\right)\right], \tag{12b}$$

$$C_2=\beta\left(\frac{e^{\delta\varphi t_0}-1}{e^{\delta t_0}-1}\right), \tag{12c}$$

$$t_0=\frac{\xi}{V_W-V_M}, V_W>V_M. \tag{12d}$$

where dimensionless coefficients C_i have been introduced for compactness.

We have effectively found a functional relationship between the material parameters that define a transportable rheology. For Doi-Edwards and Maxwell models this simplifies to a two-parameter relationship $\eta_0=f(\lambda)$. We use this expression to examine the ratio of shear stress to strain rate (as a function of relaxation time) that defines a measure of efficiency of the cilial mat in aggregate. This ratio quantity is readily obtained by dividing Eq. (5c) by the strain rate and employing the equation for η_0 [Eq. (12a)]:

$$\frac{\langle\tau\rangle}{\dot{\Gamma}_1}=\alpha\eta_0\varphi. \tag{12e}$$

When the left-hand side of Eq. (12e) is plotted as a function of the right-hand side, it may be viewed as dependent on the relaxation time. Note that $\langle\tau\rangle$ is imbedded in the expression for η_0 in Eq. (12a), but it is in fact a known quantity for a given velocity and film thickness according to Eq. (1e).

III. RESULTS

We posit that the body chooses the rheology that maximizes the stress for a given strain rate, the ratio in Eq. (12e).

(Worded conversely, the body minimizes the strain rate that must be imposed by the cilia to achieve a given stress.) This optimization can be viewed as maximizing the "efficiency" of the cilia motion in inducing mucus flow. Because relative motion is required by the cilia to induce shear stress at the mucus interface, minimizing the strain rate can be interpreted roughly as a minimization in the cilial tip velocity. It is therefore straightforward to see that this minimization would also lead to minimal power consumption by the cilial mat.

By choosing some reasonable values for the variables in the model, we plot Eq. (A1) for a few clearance velocities and active fractions in Fig. 6. For the purposes of demonstrating our model, we choose to examine only the Doi-Edwards model scenario. Experimentally acquired Jeffrey's fluid parameters, while available for comparison [29], would require that the retardation time remain variable $\lambda_{(2)}$, which complicates the optimization. This will be left to a future work.

In order to bring our predicted rheologies into agreement with experimental works, the friction coefficient μ is adjusted; this is the only parameter that appears in the final model that does not arrive from a direct experimental measurement.

An interpretation of the friction coefficient can be garnered by considering the plane shear flow of a film between a fixed wall and one moving at the average clearance velocity. In this scenario, the drag shear stress is given exactly by $\mu_{\text{eff}} V_M / h_{\text{PCL}}$, where μ_{eff} is an effective viscosity of the PCL. Thus, based on our expression [Eq. (1c)] for the drag force, the friction coefficient is defined simply as $\mu = \mu_{\text{eff}} / h_{\text{PCL}}$. For water and a PCL depth of 10 μm, the friction coefficient μ is roughly 1×10^8. Our analysis shows that μ between 1×10^7 and 1×10^9 still lead to acceptable overlap of the rheology space mapped out by our model (Fig. 7) and experimental data points. These values correspond to effective viscosities that are $0.1\times$ and $10\times$ that of water. We attribute the high end to the fact that suspensions of rodlike particles will increase the apparent viscosity of the medium [38] Alternatively, by assuming a linear profile in this back of the envelope calculation, we gloss over the complex flow profile that no doubt results from the cilial activity. Numerical estimates of the space- and time-averaged PCL flow profile have shown that the flow profile is flatter near the PCL-mucus interface, which would significantly reduce drag. [39]

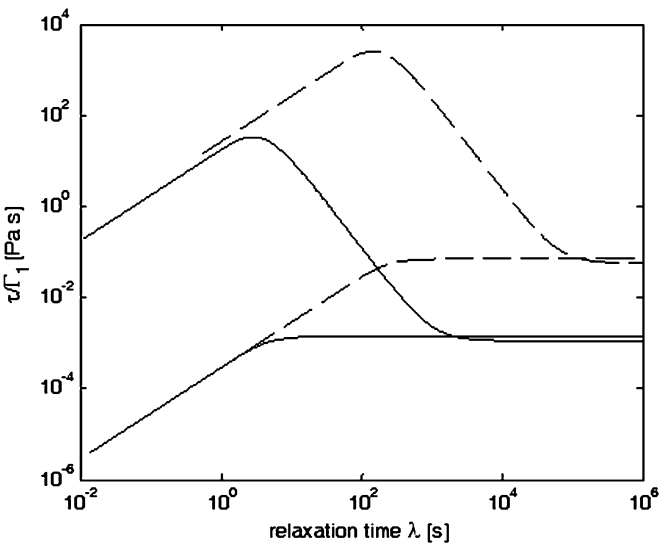

FIG. 6. $\langle\tau\rangle / \dot{\Gamma}_1$ as a function of relaxation time λ [Eqs. (12)] for a Doi-Edwards fluid for two clearance velocities $V_M = 100$ (solid lines) and 149 μm s^{-1} (dashed lines) and two active fractions $\varphi = 0.4$ and 0.5. Global maxima are only present for $\varphi \lesssim 0.5$.

TABLE II. Parameter values to be held constant in the parametric study; values are from literature if cited.

Parameter	Units	Value
Mucus thickness, h_M	m	1.0×10^{-5} [10]
Density of mucus, ρ_M	kg m^{-3}	1.0×10^3 [28]
Wavelength of metachronal wave, ξ	m	1.0×10^{-4} [10]
Velocity of metachronal wave, V_M	m s^{-1}	$(1.0 - 4.0) \times 10^{-4}$ [16]
Friction coefficient, μ	Pa s m^{-1}	$\sim 1.0 \times 10^7$ to 1.0×10^9

Figure 5 plots results for the efficacy ratio [Eqs. (12)] versus the relaxation time for a Doi-Edwards fluid (see Table I). Results show that there is a global maximum in the plots that exists only when the active fraction is less than $\sim$0.5. This seems a reasonable finding; it has been cited that the cilia spend roughly 1/3 of their beat cycle actively propelling mucus [35].

The local maximum is physically relevant as it corresponds to a rheology where the force invoked by a given cilia motion is maximized; one might expect the body to perform this maximization. By selecting the relaxation times that correspond to the peaks we can plot optimal rheology contours [Eq. (12b)] as a function of active fraction and clearance velocity (Fig. 7). By choosing a range of velocities and active fractions we see that experimentally acquired values lie in the

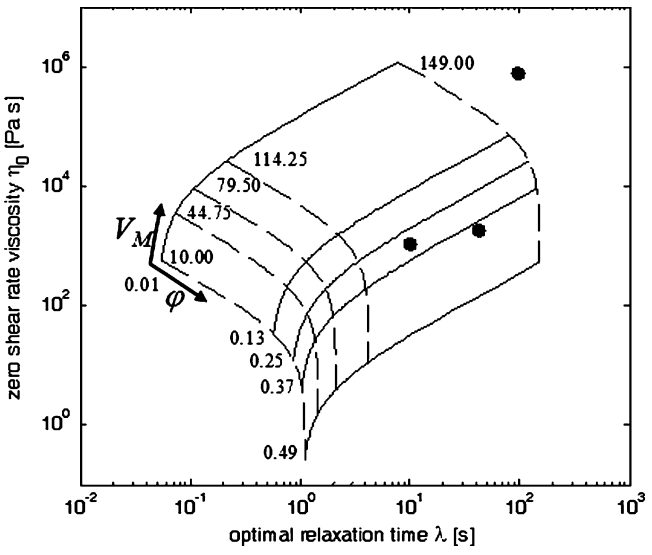

FIG. 7. Optimal rheology contours of constant active fraction (solid line) and constant clearance velocity (dashed line) [Eq. (12b) by using optimal values illustrated in Fig. 6]. All contours are evenly spaced: $\varphi \in [0.01, 0.49]$, $V_M \in [10\ 149\ \mu\text{m s}^{-1}]$. Other parameter values: $V_W = 150\ \mu\text{m s}^{-1}$, $\mu = 1 \times 10^7$ Pa s m^{-1}. The Doi-Edwards model parameters are used in this plot to allow for direct comparison with experimental values (data points) [28].

space spanned by our model. All contours are evenly space on a linear scale; thus we can see that optimal rheology changes abruptly as clearance velocity approaches that of the wave velocity (150 μm s^{-1}) and at the extrema of active fractions (0.01 and 0.49).

IV. DISCUSSION

In this paper we have developed a model for transport of a viscoelastic mucus film by considering three self-consistent analysis of the mucociliary system. Key to our work is the appropriate choice of reference frames that allow us to simplify governing equations and consider only what we posit are the most important aspects of the clearance mechanism. Our model readily reveals an optimal choice of rheology for given clearance velocity and other parameters. We are also able to demonstrate that the rheologies we predict align with those acquired experimentally. Alternatively, one could also consider the inverse problem and calculate the velocity at which a given sample can be expected to clear by using this model.

Figure 7 shows us that as the clearance velocity approaches that of the wave velocity, the relaxation time must increase. This occurs because as the similarity in velocities increases, the effectiveness of the tensile stresses to support the unstrained region as a rigid body is reduced. When the velocities are equal, "infinite" relaxation time would be required to satisfy the force balance we have constructed. The explanation is clear when the problem is viewed in a frame of reference moving with the mucus; crucial cyclic loading would not occur. In this case, mucus is either permanently in a state of strain, or never strained at all. According to our model assumptions, this situation will not allow for net tensile forces to overcome the adverse effects of friction and mucus weight, according to the analysis in Sec. II C.

We also find that decreasing the active fraction for a given clearance velocity leads to a decrease in the optimal relaxation time but also to an increase in the associated viscosity, according to Eq. (12b). That is, the mucus relaxation time is lessened despite having to effectively maintain its stress state when it has a longer unstrained region to traverse. In spite of this, the stress that is built initially during the active region is larger for two reasons: The required viscosity is larger in this scenario, and the initial stress builds faster when the relaxation time is shorter (under the Maxwell description). Thus, this result reveals the origin of the optimal rheology we observe in our model: Relaxation hinders shear stress development but prevents dissipation of stress upon which tensile forces are reliant.

An interesting consequence of our model is that it implies that mucus rheology is dependent on the generation of the respiratory tract. As available surface area for transport changes, mucus film thickness and velocity must change accordingly owing to mass conservation. Estimates of clearance velocity as a function of lung generation have been calculated by other researchers. Roughly speaking, mucus clearance velocity was found to increase in the larger airways and decrease in the finer generations of the respiratory tract [23]. Our model, in conjunction with these results, therefore predicts that mucus found in the trachea should possess a longer relaxation time and higher viscosity as compared to finer lung generations. While it is known that the mucus production capability of the respiratory tract varies with generation [40], to our knowledge generation-dependent rheological data has not explicitly examined.

By altering the one free parameter in our model, the friction coefficient, we can bring the model's optimal rheology contours (Fig. 7) into proximity of experimentally acquired rheologies. However, we note that the data points we plot are for different prepared solutions of varying mucin concentration. Therefore, all of the data points may not necessarily correspond to a naturally occurring state. Furthermore, other physiological parameters that accompany the procured samples (V_M,V_W,h_M, etc.) obviously have been assumed in this paper based on prior measurements and existing data. (i.e., we do not know the film thickness or transport velocity of the samples with which we are making our comparison in Fig. 7). These factors too can shift the contours we have shown. Yet the order-of-magnitude agreement of rheologies predicted by Eqs. (12) and existing rheological data may indicate that the correct mechanisms for bulk transport have been considered.

Our model invokes a variety of assumptions. The most severe of these is the requirement of rigid-body movement on the part of the unsupported region. This limits the model to the symplectic wave case; however, we note that mucus transport could still occur if the mucus elongated and subsequently shortened so as not to translate as a rigid body but still convect without losing fluid connectivity. Such a model could be developed in the future. It is worth noting that the experimental evidence for symplectic motion being the dominant mode of metachrony is strong [16]; it has been observed in tissues from multiple species by using high-speed video while previous conclusions of antiplectic metachrony [10] were arrived at through the examination of fixed tissues. It is also compelling that our requirement that the wave velocity must be greater than the transport velocity (arrived at in Sec. II C) concurs with the bulk of the observations in the same study where symplectic coordination was noted [16].

The initial purpose of the model was to test our postulates about how mucus relaxation time and the production of tensile forces along flow lines could benefit transport. We have constructed a model that incorporates our hypotheses of the most salient features of linear and nonlinear viscoelasticity. In the end, we show that a particular combination of viscosity and relaxation time maximizes the stress for a given rate of strain, and this metric can be used to assess the efficacy of a cilia stroke on mucus clearance. This result is intuitively pleasing, as the body must have some means of choosing what mucus rheology is best for transport. Perhaps the proposed mechanism explains in a simple manner how that is done. No doubt, more refined models can and will be generated in the future, but at this point, the level of available data precludes our ability to refine and test improvements. Our proposed mechanism is consistent with experimental data taken from a variety of sources, as seen in Fig. 7. Our model is simple to implement, and all of the parameters, save for the friction coefficient, are experimentally acquirable. We therefore hope that our description of mucociliary transport provides a framework that guides future experimental and theoretical investigations. A more rigorous validation will be possible once additional experimental data is available.

APPENDIX A: STEP RESPONSES TO THE GENERAL MODEL

In Sec. II we proposed a general linear viscoelastic model that could be solved to yield simultaneously the responses of Maxwell, Doi-Edwards, and Jeffrey's fluid models:

$$\delta\tau + \frac{d\tau}{dt} = \alpha\eta_0\left[\delta\dot{\gamma} + (1-\beta)\frac{d\dot{\gamma}}{dt}\right]. \tag{A1}$$

We begin by taking the Laplace transform of the entire expression, leaving both shear stress and the strain rate as variable functions of time:

$$\begin{aligned} L\{\tau(t),\dot{\gamma}(t)\} &= T(s),G(s) \rightarrow \delta T + (Ts - \tau_0) \\ &= \alpha\eta_0[\delta G + (1-\beta)(Gs - \dot{\gamma}_0)]. \end{aligned} \tag{A2}$$

Values for the parameters α, β, and δ were given in Table I. We assume that the strain rate is imposed, and given by

$$\dot{\gamma} = \dot{\Gamma}_1[u(t) - u(t-\varphi t_0)].$$

Note that here we are only solving for the transient component of the stress response. Superposed on this solution is a constant shear stress owing to strain rate $\dot{\Gamma}_0$. The initial condition for $\dot{\gamma}$ is given as

$$\dot{\gamma}(t=0) = \dot{\gamma}_0 = 0. \tag{A3}$$

The Laplace transform of the strain rate becomes

$$G(s) = \dot{\Gamma}_1\left(\frac{1}{s} - \frac{e^{-\varphi t_0 s}}{s}\right). \tag{A4}$$

Substituting these relationships into Eq. (A2) yields the following:

$$\begin{aligned} \delta T + (Ts - \tau_0) = \alpha\eta_0\Bigg\{&\delta\left[\dot{\Gamma}_1\left(\frac{1}{s} - \frac{e^{-\varphi t_0 s}}{s}\right)\right] \\ &+ \dot{\Gamma}_1(1-\beta)(1 - e^{-\varphi t_0 s})\Bigg\}. \end{aligned} \tag{A5}$$

Next, the Laplace transform of the shear stress $T(s)$ is solved for

$$\begin{aligned} T(s) = {}& \dot{\Gamma}_1\alpha\eta_0\delta\left(\frac{1}{s(s+\delta)} - \frac{e^{-\varphi t_0 s}}{s(s+\delta)}\right) \\ &+ (1-\beta)\dot{\Gamma}_1\alpha\eta_0\frac{(1 - e^{-\varphi t_0 s})}{(s+\delta)} + \frac{\tau_0}{(s+\delta)}. \end{aligned} \tag{A6}$$

Inverting the expression yields the shear stress as a function of time:

$$\begin{aligned} &L^{-1}\{T(s)\} \\ &= \tau_{xy}(t) \rightarrow \tau_{xy}(t) \\ &= \begin{cases} \alpha\eta_0\dot{\Gamma}_1(1 - \beta e^{-\delta t}) + \tau_0 e^{-\delta t}, & t \in [0,\varphi t_0], \\ \alpha\eta_0\dot{\Gamma}_1(-\beta + \beta e^{\varphi t_0})e^{-\delta t} + \tau_0 e^{-\delta t}, & t \in [\varphi t_0, t_0]. \end{cases} \end{aligned} \tag{A7}$$

Note that for the Jeffrey's fluid case ($\beta \neq 0$), jumps in stress are present at the beginning and end of the applied rate of strain. This is owing to the additional viscous element in the model that responds instantly to changes in applied strain.

APPENDIX B: TENSILE STRESSES IN A UNIDIRECTIONAL FLOW

In Sec. III we extended our general viscoelastic model to one that allowed, for large deformations,

$$\delta\tau + \tau_{(1)} = \alpha\eta_0\left[\delta\gamma_{(1)} + (1-\beta)\gamma_{(2)}\right]. \tag{B1}$$

For a steady, simple shear flow where $u_y, u_z = 0$, this reduces to the following [12]:

$$\begin{aligned} &\delta\begin{bmatrix} \tau_{xx} & \tau_{xy} \\ \tau_{xy} & \tau_{yy} \end{bmatrix} - \begin{bmatrix} 2\tau_{xy} & \tau_{yy} \\ \tau_{yy} & 0 \end{bmatrix}\frac{\partial u_x}{\partial y} \\ &= \alpha\eta_0\left\{\delta\begin{bmatrix} 0 & \frac{\partial u_x}{\partial y} \\ \frac{\partial u_x}{\partial y} & 0 \end{bmatrix} - (1-\beta)\begin{bmatrix} 2\left(\frac{\partial u_x}{\partial y}\right)^2 & 0 \\ 0 & 0 \end{bmatrix}\right\}. \end{aligned} \tag{B2}$$

In this scenario, each component of the stress tensor can be stated in terms of the strain rate:

$$\tau_{xx} = \frac{2\alpha\eta_0(\beta-1)}{\delta}\left(\frac{\partial u_x}{\partial y}\right)^2 + \frac{2}{\delta}\frac{\partial u_x}{\partial y}\tau_{xy}, \tag{B3}$$

$$\tau_{yy} = 0, \tag{B4}$$

$$\tau_{xy} = \alpha\eta_0\frac{\partial u_x}{\partial y}. \tag{B5}$$

By combining these relationships between stress and strain rate with momentum conservation equations in the x and y directions, we get

$$\rho\left(\frac{\partial u_x}{\partial t} + u_x\frac{\partial u_x}{\partial x} + u_y\frac{\partial u_x}{\partial y}\right) = \frac{-\partial P}{\partial x} + \frac{\partial\tau_{xy}}{\partial y} + \frac{\partial\tau_{xx}}{\partial x}, \tag{B6}$$

$$\rho\left(\frac{\partial u_y}{\partial t} + u_x\frac{\partial u_y}{\partial x} + u_y\frac{\partial u_y}{\partial y}\right) = \frac{-\partial P}{\partial y} + \frac{\partial\tau_{xy}}{\partial x} + \frac{\partial\tau_{yy}}{\partial y}, \tag{B7}$$

and simplifying for unidirectional flow we have

$$\alpha\eta_0\frac{\partial^2 u_x}{\partial y^2} = 0, \tag{B8}$$

$$\frac{\partial P}{\partial y} = 0. \tag{B9}$$

We assume that there is no pressure gradient in the direction of flow because there is negligible pressure drop in the free stream over the length scale of interest. Thus, according to Eq. (B8), the strain rate and shear stress must be constant within the film. Because the stress is fixed at the PCL-mucus interface and must be constant throughout the cross section, from Eq. (B5), the strain rate must then be

$$\frac{\partial u_x}{\partial y} = \frac{\tau_{xy}}{\alpha\eta_0}. \tag{B10}$$

This leads to the result that we seek, which is the normal stress distribution in terms of the shear stress distribution:

$$\tau_{xx} = \frac{2\beta}{\delta\alpha\eta_0}\tau_{xy}^2. \tag{B11}$$

[1] M. A. Chilvers and C. O'Callaghan, Paediatr. Respir. Rev. **1**, 27 (2000).
[2] J. R. Blake, J. Fluid Mech. **46**, 199 (1971).
[3] J. R. Blake, J. Fluid Mech. **49**, 209 (1971).
[4] J. Blake, J. Fluid Mech. **55**, 1 (1972).
[5] S. R. Keller, T. Y. Wu, and C. Brennen, *Proceedings of the Symposium on Swimming and Flying in Nature* (California Institute of Technology, Paśadena), pp. 253–271.
[6] G. R. Fulford and J. R. Blake, J. Theor. Biol. **121**, 381 (1986).
[7] S. M. Ross and S. Corrsin, J. Appl. Phys. **37**, 333 (1974).
[8] E. Lauga, Phys. Fluids **19**, 083104 (2007).
[9] O. S. Pak, T. Normand, and E. Lauga, Phys. Rev. E **81**, 036312 (2010).
[10] M. J. Sanderson and M. A. Sleigh, J. Cell Sci. **47**, 331 (1981).
[11] D. J. Smith, E. A. Gaffney, and J. R. Blake, Proc. R. Soc. London, Ser. A **465**, 2417 (2009).
[12] R. B. Bird, *Dynamics of Polymeric Liquids* (Wiley, New York, 1987).
[13] R. H. Dillon, L. J. Fauci, and X. Z. Yang, Comput. Math. Appl. **52**, 749 (2006).
[14] R. H. Dillon, L. J. Fauci, C. Omoto, and X. Yang, Ann. N.Y. Acad. Sci. **1101**, 494 (2007).
[15] S. M. Mitran, Computers Struct. **85**, 763 (2007).
[16] M. Ryser, A. Burn, T. Wessel, M. Frenz, and J. Rička, Eur. Biophys. J. Biophys. Lett. **37**, 35 (2007).
[17] L. B. Wong, I. F. Miller, and D. B. Yeates, J. Appl. Physiol. **75**, 458 (1993).
[18] R. A. Gelman and F. A. Meyer, Am. Rev. Resp. Disease **120**, 553 (1979).
[19] G. Lorenzi, G. M. Böhm, and E. T. Guimarães, M. A. Vaz, M. King, and P. H. Saldiva, Biorheology **29**, 433 (1992).
[20] G. T. Yates, T. Y. Wu, R. E. Johnson, A. T. W. Cheung, and C. L. Frand, Biorheology **17**, 151 (1980).
[21] Z. Teff, Z. Priel, and L. A. Gheber, Biophys. J. **92**, 1813 (2007).
[22] Z. Teff, Z. Priel, and L. A. Gheber, Biophys. J. **94**, 298 (2008).
[23] B. Asgharian, W. Hofmann, and F. J. Miller, J. Aerosol Sci. **32**, 817 (2001).
[24] H. Winet and J. R. Blake, Biorheology **17**, 135 (1980).
[25] H. Winet *et al.*, Progress Clinical Biological Res. **80**, 29 (1982).
[26] H. Winet *et al.*, J. Appl. Physiol. **56**, 785 (1984).
[27] H. Winet, Biorheology **24**, 635 (1987).
[28] G. J. Besseris and D. B. Yeates, J. Chem. Phys. **127**, (2007).
[29] S. S. Davis and J. E. Dippy, Biorheology **6**, 11 (1969).
[30] M. King and P. T. Macklem, J. Appl. Physiol. **42**, 797 (1977).
[31] M. King, Biorheology **17**, 249 (1980).
[32] S. H. K. Trindade *et al.*, Int. J. Pediatric Otorhinolaryngology **72**, 581 (2008).
[33] J. R. Blake and G. R. Fulford, Physicochem. Hydrodynam. **5**, 401 (1984).
[34] M. A. Sleigh, J. R. Blake, and N. Liron, Am. Rev. Resp. Disease **137**, 726 (1988).
[35] J. R. Blake and M. A. Sleigh, Bio. Rev. Cambridge Philos. Soc. **49**, 85 (1974).
[36] D. J. Smith, E. A. Gaffney, and J. R. Blake, Respiratory Physiol. Neurobiol. **163**, 178 (2008).
[37] R. H. Ewoldt, A. E. Hosoi, and G. H. McKinley, Abstr. Pap. Am. Chem. Soc. **231**, 387 (2006).
[38] H. A. Barnes, J. F. Hutton, and K. Walters, *An Introduction to Rheology* (Elsevier, New York, 1989).
[39] J. R. Blake and H. Winet, Biorheology **17**, 125 (1980).
[40] M. A. Grippi, *Pulmonary Pathophysiology* (Lippincott, Philadelphia, 1995).